Two Dimensional X-Ray Diffraction (2D-XRD) studies on Olivine of U.S.A.

[1]SALMA JABEEN*, [1]SYED MOHSIN RAZA, [1]MUHAMMAD ASHFAQ AHMED,
[2]MASOOM YASIN ZAI AND [3]KURT ERLACHER
[1]Department of Physics, University of Balochistan, Quetta-87300, Pakistan.
*sjabeen_Phy@yahoo.com**
[2]Institute of Biochemistry, University of Balochistan, Quetta-87300, Pakistan.
[3]XRD Division Bruker's Labs, Germany.

(Received on 8th February 2010, accepted in revised form 23rd December 2010)

Summary: The Olivine (Mg, Fe) 2SiO4 of USA has been studied with two dimensional X-ray diffracto meter (D8 discover with GADDS). The two distinct phases of orthorhombic structure, one with Mg_8 [Fe_2 SiO_4] and the other with Mg_2 SiO_4 is observed. We also observed phase transitions due to presence of iron and Silicon preferably the structural change of Mg_8[Fe_2 SiO_4] from orthorhombic to spinnel like (spinnel chord) structure. Magnesium ions in Mg_8[Fe_2 SiO_4] shuffle, arrange at the five vertices of a pentagon and the remaining three at the central but with displaced position from the plane of the pentagon, Thus resulting into a three dimensional spinnel chord like structure. We evidenced the same from diverse orientations of phase peaks and indeed from Kossel lines.

Introduction

The mineral liberation analysis (MLA) is a paradigm for applied mineralogy and metallurgical processing. The intrinsic parameters of ores used in processing plant design are imperative. For the progress of an accurate, speedy and user supporter mineral liberation analyzer, the most popular and widely used method for material analysis is X-ray diffraction (XRD) technique [1-6].

The methods and techniques used in the " Mineral Liberation analyzer(MLA)", consisting of a specially developed soft-ware package and a standard modern scanning electron microscopy(SEM),fitted with a energy dispersive spectrum(EDS)analyzer, on ore samples was presented by Ying Gu [7]. Velasquez Pablo *et al.* presented a chemical morphological and electrochemical analysis of electrochemically modified electrode surfaces of natural ors in alkaline solutions [8]. The layer morphology and structural properties of FeS_2(pyrite)thin films, grown on natural Pyrite and synthetic ZnS crystals by scanning electron microscope(SEM)and X-ray diffractions ,etc were studied by Thomas *et al.* [9]. J.S.Nkoma and G. Ekosse performed the energy-dispersive X-ray spec-troscopy (EDS) of Cu-Ni ore-bodies from different mines of Botswana for mineral characterization and elements special relationships with the use of X-ray diffraction (XRD) technique [10, 11].

Junqing *et al.* analyzed their samples by using X-ray powder diffraction and transmission electron microscope (TEM) results [12, 13]. S. M. Raza *et al.* studied the Genesis of mineral rocks of pyrite and chalcopyrite of Balochistan, Pakistan with EPMA (electron probe microanalysis), SEM (Scanning electron microscopy) EDS (Electron dispersive studies) and MLA (Mineral liberation analysis) techniques [14].

Salma Jabeen *et al.,* studied the dolomite of Balochistan (Pakistan) by using dynamic temperature X-ray diffraction (DTXRD) technique [15]. Salma Jabeen, S. M. Raza *et al.* presented the analysis of dolomite of Balochistan(Pakistan) by using X-ray fluorescence spectroscopy (XFS), Simultaneous differential thermal analysis (SDTA), Thermogravimetric analysis(TGA)and differential scanning calorimetry(DSC) [16].

Olivine is most commonly found in basalts. We used amorphous Olivine (Mg, Fe) $2SiO_4$ obtained from U.S.A and performed 2DXRD studies on the Ore Samples. The Olivine also called Forsterite occurs with regards of Geological setting in mafic and ultramafic igneous rocks, meta morphosed impure dolomites. For Physical properties of Forsterite section, its Lustre is vitreous; Hardness is 7, Tenacity Brittle, Density 3.275g / cm^3. Forsterite crystal system is Orthorhombic with cell a=4.754A^0, b=10.1971 A^0, c=5.9806 A^0 with unit cell V289.92 A^{0^3}. Olivine morphology is Euhedral to subhedral crystals with Twinning {100} {011} {012} [17]. For X-ray diffraction, the suitable radiation for Olivine (Forsterite) is Copper K_α.

*To whom all correspondence should be addressed.

Minerals in the Olivine group crystallize in the orthorhombic system (space group pbnm) with isolated silicate tetrahedral, meaning that Olivine is a mesosilicate. In an alternative view, the atomic structure can be described as hexagonal, closed-packed array of oxygen ions with half of the octahedral sites occupied with magnesium or iron ions and one-eighth of the tetrahedral sites occupied by silicon ions. Olivine is not radioactive. C.S Barritt studied crystallography in detail [18].

Result and Discussions.

Fig. 1 Shows 2DXRD pattern of Olivine $Mg_8[Fe_2SiO_4]$. Fig. 2. Shows 2DXRD pattern for Phi-rotation in steps of 5^0. Phi rotation corresponds to azimuthal angle variations with Φ rotations in steps of 5^0 up to 95^0 .We can see orientations of polycrystals especially with Wolf Net.

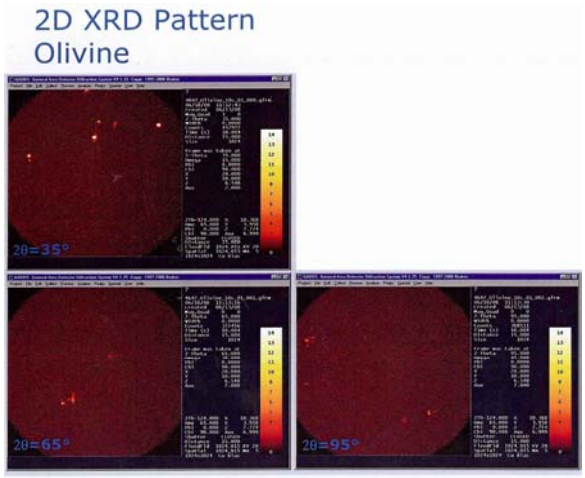

Fig. 1: Shows 2DXRD pattern of Olivine.

With $\Phi = 30^0$ to 45^0 and $\Phi = 60^0$ to 65^0, we observe more orientations of orthorhombic crystallites of Olivine. Greinger's chart helps to determine the orientation of single crystals with diverse symmetries, folded and embedded structures. All the spots shown in these frames are Von Laue spots. Omega (Ω) is the solid angle with which reflections from crystallites are observed.

$2\theta = 65^0$ is the optimum value at which maximum reflections occur.Fig. 3 shows 2DXRD pattern Olivine phi-rotation. Kossel lines are evident with Φ rotation of 0^0 to 360^0 at each 2θ positions. Each Kossel line is a representative of peak position in diffractometer at different 2θ values.

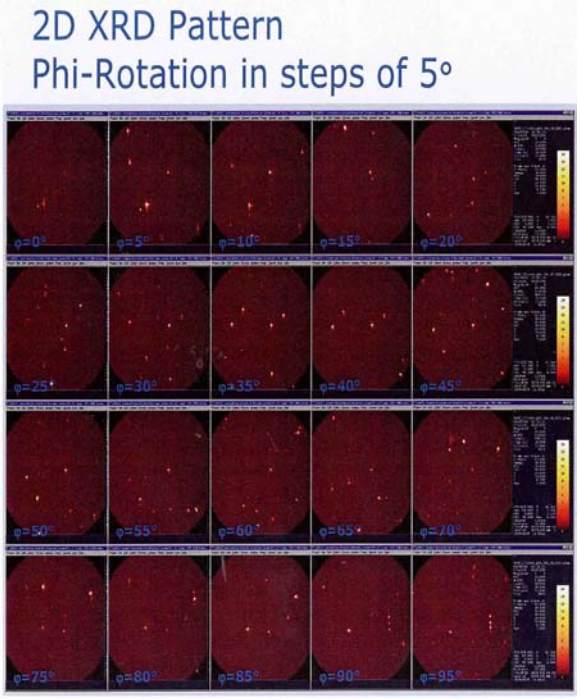

Fig. 2: Shows 2DXRD pattern phi-rotation in steps of 5^0.

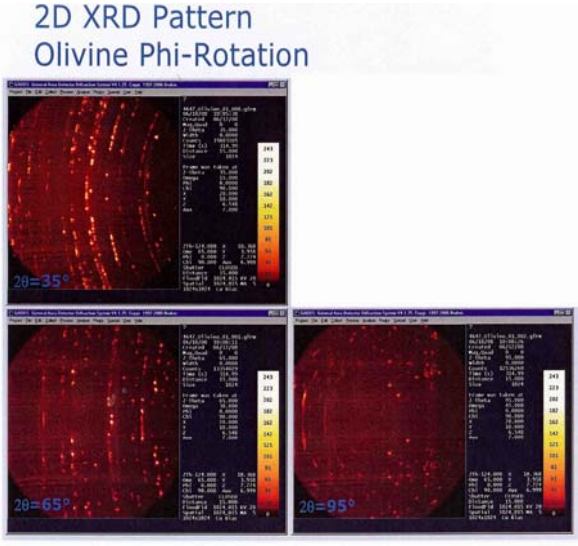

Fig. 3: Shows 2DXRD pattern Olivine phi-Rotation.

Kossel lines are distinct especially with $2\theta = 65^0 \Rightarrow \theta = 32.5^0$.

We calculated the'd' that is displaced position of magnesium ions by using the formula,

$$2d\sin\theta = n\lambda \text{ L L } \rightarrow (1)$$

For $n=1, \theta = 32.5$ *and* $\lambda = Cuk_{\alpha} = 1.54\times10^{-10} m.$

$$d = 1.44\times10^{-10} m.$$

with deformed Kossel line(less curvature); we calculated 'd' which is a proof for structural change. This'd' is an optimum that is maximum displacement of magnesium ions.

Fig. 4 shows the phase identification with DIFFRAC ^{plus} EVA. Phase identification shows the presence of two phases of orthorhombic Olivine. Fig. 5 shows the phase identification with DIFFRAC ^{plus} EVA. We chose 4-peak positions for our calculations and used the formula (1) for first order spectrum with n=1.We calculated θ for peak positions by using formula:

$$2\theta = X \Rightarrow \theta = \frac{X}{2} \text{ L L } \rightarrow (2)$$

All details are explained in Table-1. Fig. 6 shows the phase identification with DIFFRAC ^{plus} EVA. DIFFRAC ^{plus} EVA favours two different Olivine's one with $Mg_8[Fe_2SiO_4].$ and the other with Mg_2Sio_4. Fig. 7 shows the identification of these two phases with DIFFRAC ^{plus} EVA. The zoomed region in the lower two theta range is shown for better match between the diffraction pattern and the identified Olivine phase. Fig. 8 presents the phase identification with DIFFRAC ^{plus} EVA. Fig. 8 explains the indication of different crystalline orientations with in the sample with the variations in peak heights. Fig. 8 also shows two distinct phase transitions, one on the left with Mg_2Sio_4 phase and the other on the right with $Mg_8[Fe_2SiO_4].$ phase. Fig. 9 shows the three Bravais lattices. All these three Bravais lattices are found in our Olivine. Diffractograms show the existence of all three Bravais lattices of orthorhombic structure in Olivine found at different places.

Fig. 10 shows the Peridot (Forsterite) recrystallized at the base for location: Skardu, Nooristan, Pakistan. Table-1 explains the behavior of d_1, d_2, d_3 and d_4 with the variation of the selected peak positions for 1st and 2nd phase very well.Table-1 shows that the 1st phase $Mg_8[Fe_2SiO_4].$ with primitive, base centered, body centered and face centered orthorhombic structure.

From the above discussion we conclude that deformation in the crystallization is occurring inside the selected sample, as is evident from Fig. 8. The results show single reflections from mono crystalline regions. The orientations of these mono crystalline domains strongly vary over the sample surface. It is also possible to evaluate the orientation of the crystal domains. The D8 discover with GADDS allows very fast on line-measurements due to the high sensitivity of HI-STAR (2D-detector). Each diffraction image (frame) of the HI-STAR detector covers the information of many diffraction spots in a large angular range.

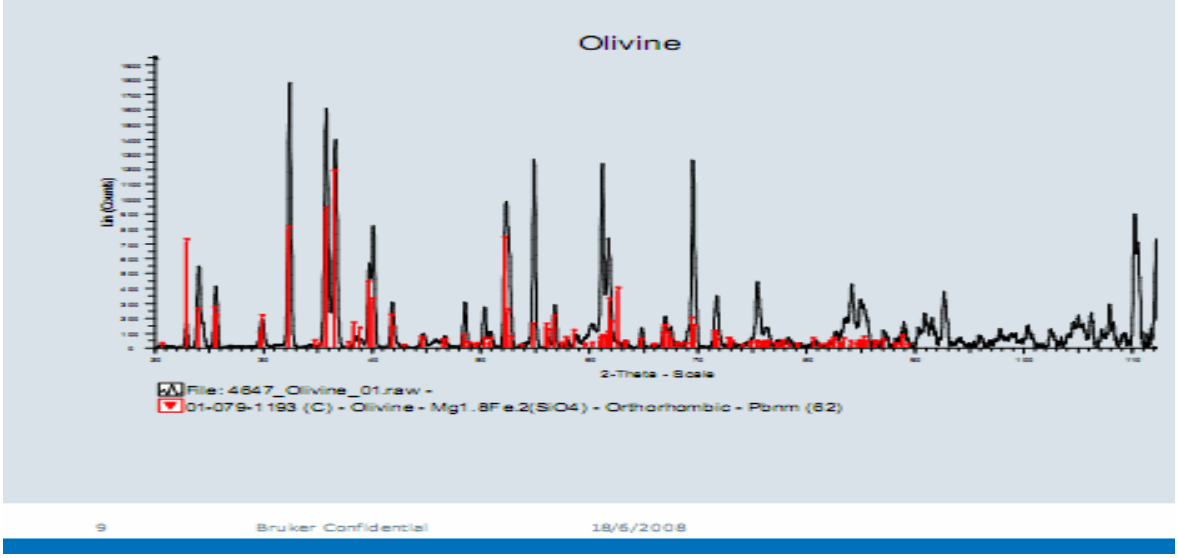

Fig. 4: Shows phase identification with DIFRAC^{plus} EVA.

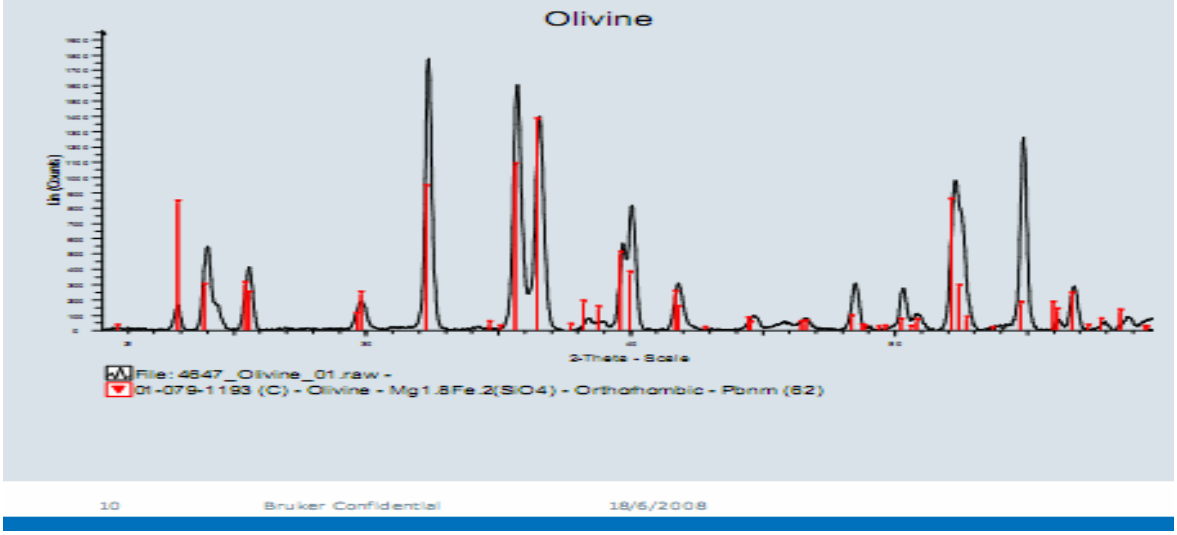

Fig. 5: Shows phase identification with DIFRAC^{plus} EVA.

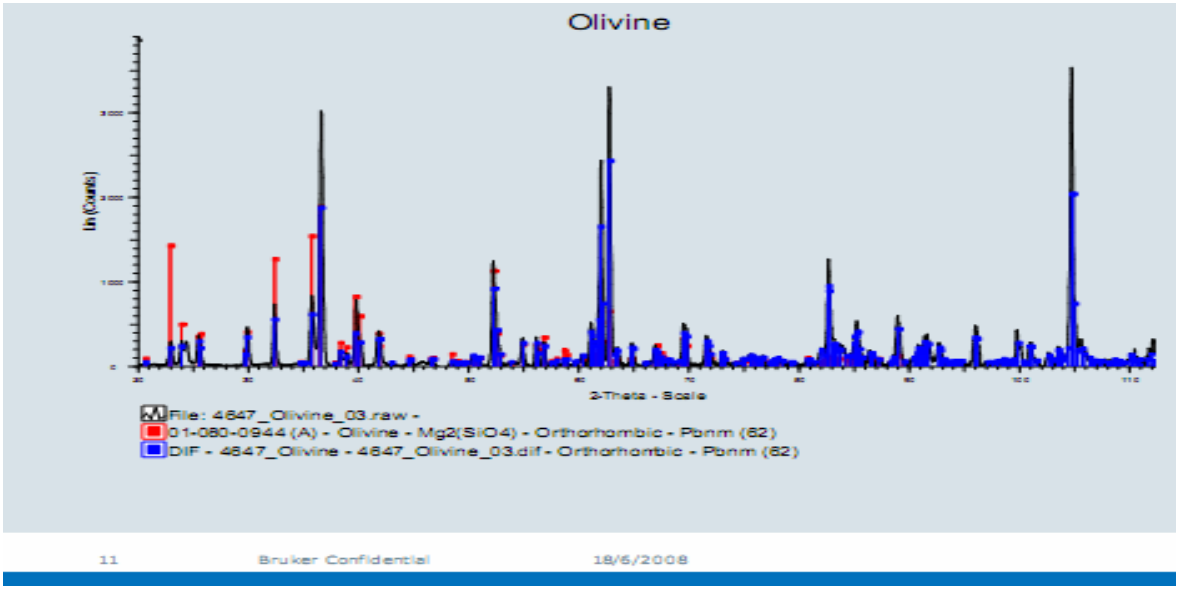

Fig. 6: Shows phase identification with DIFFRAC^{plus} EVA.

Table-1: Shows the related important parameters calculated from the peak-Positions.

S. No.	Observed – Phases.	Peak Position.	$2\theta = X$ $\theta = \frac{X}{2}$	$d = \frac{\lambda}{2\sin\theta} m$
1.	**First-Phase** **Olivine** $\left(Mg_8\left[Fe_2SiO_4\right]\right)$ **Some of the crystallites Of first phase are Deformed.**	**1st**	$\theta_1 = 16.15$	$d_1 = 3\times10^{-10}$ **m**
2.		**2nd**	$\theta_2 = 17.8$	$d_2 = 2.516\times10^{-10}$ **m**
3.		**3rd**	$\theta_3 = 18.2$	$d_3 = 2.464\times10^{-10}$ **m**
4.	d_4 **corresponds to position of Magnesium ion base-centered Body centered and face centered Orthorhombic structure.**	**4th**	$\theta_4 = 27.4$	$d_4 = 1.674\times10^{-10}$ **m**

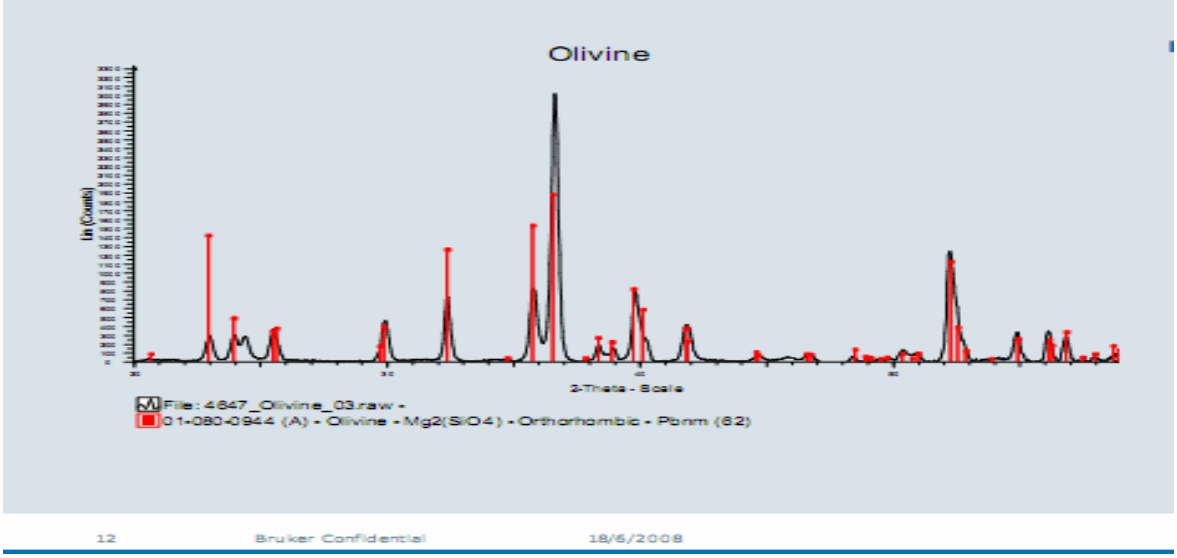

Fig. 7: Shows phase identification with DIFFRAC^{plus} EVA.

Table-2: Shows the related important parameters calculated from the peak– Positions.

S. No	Observed – Phases.	Peak Position	$2\theta = X$ $\theta = \frac{X}{2}$	$d = \frac{\lambda}{2\sin\theta} m$
1.	**Second-Phase Olivine** (Mg_2Sio_4) **The Second phase is not Deformed.**	1st	$\theta_1 = 11.5$	$d_1 = 0.07\times10^{-10}$ m
2.		2nd	$\theta_2 = 16.2$	$d_2 = 3\times10^{-10}$ m
3.		3rd	$\theta_3 = 17.9$	$d_3 = 2.52\times10^{-10}$ m
4.	d_4 **also corresponds to position of Magnesium ions of base-centered Body centered and face centered Orthorhombic structure.**	4th	$\theta_4 = 18.3$	$d_4 = 2.45\times10^{-10}$ m

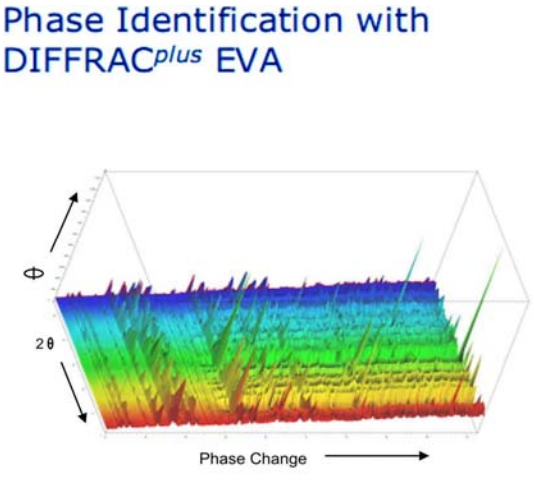

Fig. 8: Shows Phase identification with DIFFRAC^{plus} EVA.

Experimental

We performed experimental analysis for Olivine with Diffractomete D8 discover with GADDS. To cover a large 2 theta range 3 2D frames were collected at the specified measurements position. A 0.8 mm pinhole collimator was used. Measurement time per frame was 10 second. During experiment we collected 2DXRD patterns with phi-rotation in steps of 5^0. The frames show the diffraction pattern at different phi positions starting from phi=0^0 to phi=95^0. 2 theta was 65^0 and Omega (Ω) was 30^0. Measurement time per frame was 10 second. For phase identification we average over multiple orientations. Therefore, a continuous phi rotation of 360^0 was performed during data collection at each 2θ position. To cover a large 2θ range 32D frames were collected at increasing 2θ values. A

0.8mm pinhole collimator was used. Measurement time per frame was 315 second.

For phase identification we utilized DIFFRAC ^{plus} EVA and took the merged diffraction pattern of the 3 frames and hence show the presence of Olivine. For reasonable match we entered the various entries of Olivine within the pdf 2 data base and got the result of Fig. 4.We took the Zoomed region in the lower 2 theta range to better show the good match between the diffraction pattern and the identified phase and got the results shown in Fig. 5 for $Mg_8[Fe_2SiO_4]$.

For different Olivine phase identification we utilized DIFFRAC ^{plus} EVA and took the merged diffraction pattern of the 3 frames at a different position on the sample. The data base entry of the selected Olivine phase only contains data up to 2theta=90^0. From this data base we took the crystal information and calculated the peak positions for higher 2 theta values. We took the notable excellent peak positions of this calculated pattern at high 2 theta angles shown in Fig. 6. We took the Zoomed region in the lower 2theta range to better show the good match between the diffraction pattern and the identified Olivine Mg_2Sio_4 phase shown in Fig. 7.

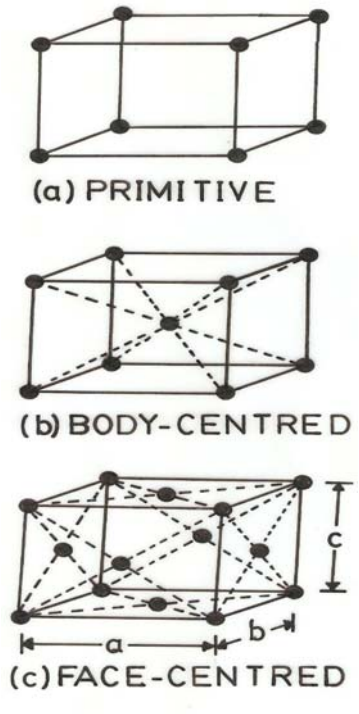

Fig. 9: Shows the basic information of three Bravasis lattices.

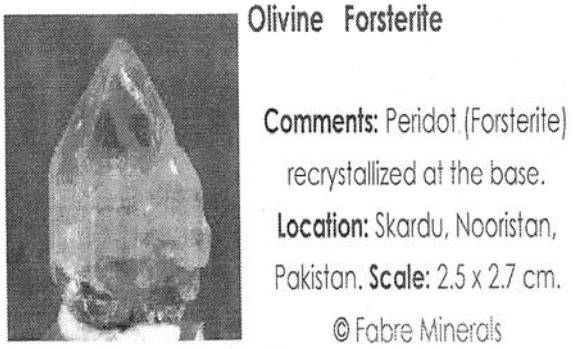

Fig. 10: Shows the recrytalization of Olivine Forsterite at the base.

Finally we took the diffraction pattern of 55 different sample positions (Grid of 11×5mm with step width of 1mm) of the Olivine sample and hence got the variations in peak heights indicated different crystalline orientations with in the sample shown in Fig. 8.

Conclusions

We infer from this study the following conclusions.

1. The Kossel lines are evident with Φ rotation of 0^0 to 360^0 at each 2θ positions and distinct especially with $2\theta = 65^0$.
2. With Kossel lines (partially deformed that loss of curvature) and Fig. 5, it is evident that the orthorhombic phase $Mg_8[Fe_2SiO_4]$ is deformed into a spinnel chord like structure.
3. From figure 4 and 7 the two phases of Olivine with orthorhombic structure are found, one with $Mg_8[Fe_2SiO_4]$ and the other with Mg_2Sio_4.
4. From Fig. 8 variations in peak heights indicates different crystalline orientations with in the sample. One on the left side for Mg_2Sio_4 and the other on right side for $Mg_8[Fe_2SiO_4]$ confirm.
5. The sample shows strong single reflections from monocrystalline regions.
6. The orientations of these mono crystalline domains strongly vary over the sample surface.
7. The gap on left and right sides of Fig. 8 is an indication of a deformed structure that is of orthorhombic $Mg_8[Fe_2SiO_4]$.

Acknowledgements

We are grateful to Dr. Gulam Nabi the Chairman of Geology department, University of Balochistan for his help in the collection of samples,

providing useful information and Syed Mohammad Hussain Bana International for his help to access the Laboratory support.

References

1. M. N. Aamir, M. Ahmad, N. Akhtar, G. Murtaza, M. Asadullah, *Journal of the Chemical Society of Pakistan*, **32**, 180 (2010).
2. S. Akbar, *Journal of the Chemical Society of Pakistan*, **32**, 592 (2010).
3. F. Ahmed, M. A. Abbasi, Aziz-Ur-Rehman, M. A. Awan, M. A. Iqbal, S. A. Yousaf, M. J. Iqbal, V. U. Ahmad, *Journal of the Chemical Society of Pakistan*, **32**, 277 (2010).
4. M. P. Jones, "Applied mineralogy: a quantitative approach", London: Norwell, MA, Graham and Trot man (1987).
5. W. Pet Rock, "Applied Mineralogy in the mining industry" Amsterdam, New York, Elsevier Science BV (2000).
6. R. P. King, Basic image analysis for mineralogy, in ICAM, 93 Demonstration workshop manual, pp.119-139 (1993).
7. GU Ying, *Journals of Minerals and Materials Characterization and Engineering*, **2**, 33 (2003).
8. P. Velasquez, D. M. Leinen, J. Pascual, Ramos-Barrado, R. Jose, P. Grez, H. Gomez, R. Schrebler, R. R. Del and R. Cordova; *Journal of Physical Chemistry* B, **109**, 4977 (2005).
9. B. Thomas, J. Ellmer, M. Mueller, C. Hoepfner, S. Fiechter, H. Tributsch; J.cryst.
10. J. S. Nkoma and G. Ekosse, *Journal of Physics: Condensed Matter*, **11**, 121 (1999).
11. H. U Junqing and L. U Qingyi, *Inorganic Chemistry Communications*, **2**, 569 (1999).
12. H. U. Junqing, L. U. Qingyi, T. Kaibin, Q. Yitai, Z. Guien and L. Xianming; *Journal of Materials Research*, **14**, 3870 (1999).
13. S. M. Raza, S. M. M. R. Naqvi, S. Rizvi, S. Dabir, H. Rizvi, K. Mahmood, Proc.10th International Symposum on Advanced materials, pp-77-79 (2007).
14. S. Jabeen, S. M. RAZA and G. Vanhoyland, *Journal of the Chemical Society of Pakistan*, **30**, (2008).
15. S. Jabeen, S. M. Raza, K. Mehmood, S. Atiq and Z. U. H. Farooqi, *Journal of the Chemical Society of Pakistan*, **31**, , (2009).
16. J. D. Birle, G. V. Gibbs, P. B. Moore and J. V. Smith, *American Mineralogist*, **53**, 807 (1968).
17. A. G. Nord, H. Annersten and A. Filippidis, *American Mineralogist*, **67**, 206 (1982).
18. Barret, X-ray Crystallography on Mineral ores, published: Francis and Taylor, London, 25th Edition (1986).